

Abundance of mass 47 CO₂ in urban air, car exhaust, and human breath

Hagit P. Affek*, John M. Eiler

Division of Geological and Planetary Sciences, California Institute of Technology, MC100-23, Pasadena, CA 91125, USA

Received 27 January 2005; accepted in revised form 16 August 2005

Abstract

Atmospheric carbon dioxide is widely studied using records of CO₂ mixing ratio, $\delta^{13}\text{C}$ and $\delta^{18}\text{O}$. However, the number and variability of sources and sinks prevents these alone from uniquely defining the budget. Carbon dioxide having a mass of 47 u (principally $^{13}\text{C}^{18}\text{O}^{16}\text{O}$) provides an additional constraint. In particular, the mass 47 anomaly (Δ_{47}) can distinguish between CO₂ produced by high temperature combustion processes vs. low temperature respiratory processes. Δ_{47} is defined as the abundance of mass 47 isotopologues in excess of that expected for a random distribution of isotopes, where random distribution means that the abundance of an isotopologue is the product of abundances of the isotopes it is composed of and is calculated based on the measured ^{13}C and ^{18}O values. In this study, we estimate the $\delta^{13}\text{C}$ (vs. VPDB), $\delta^{18}\text{O}$ (vs. VSMOW), δ_{47} , and Δ_{47} values of CO₂ from car exhaust and from human breath, by constructing 'Keeling plots' using samples that are mixtures of ambient air and CO₂ from these sources. δ_{47} is defined as $(R^{47}/R_{\text{std}}^{47} - 1) \times 1000$, where R_{std}^{47} is the R^{47} value for a hypothetical CO₂ whose $\delta^{13}\text{C}_{\text{VPDB}} = 0$, $\delta^{18}\text{O}_{\text{VSMOW}} = 0$, and $\Delta_{47} = 0$. Ambient air in Pasadena, CA, where this study was conducted, varied in [CO₂] from 383 to 404 $\mu\text{mol mol}^{-1}$, in $\delta^{13}\text{C}$ and $\delta^{18}\text{O}$ from -9.2 to -10.2‰ and from 40.6 to 41.9 ‰ , respectively, in δ_{47} from 32.5 to 33.9 ‰ , and in Δ_{47} from 0.73 to 0.96 ‰ . Air sampled at varying distances from a car exhaust pipe was enriched in a combustion source having a composition, as determined by a 'Keeling plot' intercept, of $-24.4 \pm 0.2\text{‰}$ for $\delta^{13}\text{C}$ (similar to the $\delta^{13}\text{C}$ of local gasoline), $\delta^{18}\text{O}$ of $29.9 \pm 0.4\text{‰}$, δ_{47} of $6.6 \pm 0.6\text{‰}$, and Δ_{47} of $0.41 \pm 0.03\text{‰}$. Both $\delta^{18}\text{O}$ and Δ_{47} values of the car exhaust end-member are consistent with that expected for thermodynamic equilibrium at $\sim 200\text{ °C}$ between CO₂ and water generated by combustion of gasoline–air mixtures. Samples of CO₂ from human breath were found to have $\delta^{13}\text{C}$ and $\delta^{18}\text{O}$ values broadly similar to those of car exhaust–air mixtures, -22.3 ± 0.2 and $34.3 \pm 0.3\text{‰}$, respectively, and δ_{47} of $13.4 \pm 0.4\text{‰}$. Δ_{47} in human breath was $0.76 \pm 0.03\text{‰}$, similar to that of ambient Pasadena air and higher than that of the car exhaust signature.

© 2005 Elsevier Inc. All rights reserved.

1. Introduction

The budget of atmospheric CO₂ is widely studied using records of mixing ratio, $\delta^{13}\text{C}$ and $\delta^{18}\text{O}$, combined with estimates of $\delta^{13}\text{C}$ and $\delta^{18}\text{O}$ values associated with CO₂ fluxes (Ciais et al., 1995a,b, 1997; Cuntz et al., 2003; Francey and Tans, 1987; Francey et al., 1995; Peylin et al., 1999). In particular, $\delta^{13}\text{C}$ values are primarily used to partition marine from terrestrial photosynthesis (Ciais et al., 1995a,b; Francey et al., 1995) and $\delta^{18}\text{O}$ values are used primarily to separate terrestrial net photosynthesis from soil

respiration (Ciais et al., 1997; Peylin et al., 1999; Yakir and Wang, 1996).

However, the number and variability of sources and sinks prevents these alone from uniquely defining the budget. For example, $\delta^{13}\text{C}$ values of respired CO₂ and CO₂ generated by combustion of oil, gasoline or biomass are effectively indistinguishable from one another. Previous efforts to separate their relative contributions to air using the $\delta^{18}\text{O}$ of CO₂ have suffered from a paucity of data, and have resorted to the assumption that combustion sources are equal atmospheric O₂ in $\delta^{18}\text{O}$ (Pataki et al., 2003a; Zimnoch et al., 2004).

CO₂ having a mass of 47 u (mainly $^{13}\text{C}^{18}\text{O}^{16}\text{O}$) provides an additional potential constraint on the atmospheric budget of carbon dioxide, but little is known in detail about its ability to differentiate among various budget components. Theoretical calculations and initial results suggest that

* Corresponding author. Fax: +1 626 683 0621.

E-mail addresses: hagit@caltech.edu (H.P. Affek), eiler@gps.caltech.edu (J.M. Eiler).

the mass 47 anomaly (Δ_{47}) value of CO_2 , a measure of the excess (or deficit, if negative) of mass 47 isotopologues, relative to the abundance predicted for a random distribution of isotopes (a detailed definition is given below), is temperature dependent (Eiler and Schauble, 2004; Wang et al., 2004) and therefore might distinguish between high temperature processes, such as combustion, vs. low temperature processes, such as respiration.

In this study, we report the isotopic composition, including mass 47 isotopologues, of CO_2 in car exhaust and in air from an urban setting (Pasadena, CA), using a ‘Keeling plot’ approach (Keeling, 1958, 1961). We then compare this combustion source to the isotopic composition of CO_2 in human breath, taken as an example of low temperature respiratory processes.

2. Methods

2.1. Air sampling and CO_2 extraction

Air was sampled at a flow rate of 1 L min^{-1} through a $\text{Mg}(\text{ClO}_4)_2$ trap into pre-evacuated 5-L glass flasks. The $\text{Mg}(\text{ClO}_4)_2$ trap reduced the moisture content in car exhaust from approximately 80% relative humidity to 1–2% (measured using a Li-Cor 1400-104 relative humidity sensor). ‘‘Ambient’’ air was sampled in the campus of the California Institute of Science (Caltech) in Pasadena, CA, between April and July 2004, always at 10 am. Samples were obtained from a third floor balcony of the North Mudd building on the Caltech campus (34.1365°N , 118.1275°W). These samples invariably contain a small, variable fraction (ca. $15\text{--}30 \mu\text{mol mol}^{-1}$) of CO_2 from local fossil-fuel sources (Newman et al., 1999). ‘‘Traffic’’ air was sampled at a time of relatively heavy traffic (8 am) at street level at the intersection of E. California and S. Wilson in Pasadena, CA (34.1360°N , 118.1279°W). ‘‘Exhaust’’ air was sampled at distances of 5–200 cm from the exhaust pipe of either of two cars (most samples are exhaust from a 2001 Ford Taurus; the others are from a 1991 Jeep Cherokee; Table 1). Samples of ‘‘ambient,’’ ‘‘traffic,’’ and ‘‘exhaust’’ air were used in a ‘Keeling plot’ analysis to characterize the isotopic composition of the car exhaust end-member. Samples were collected over the course of 1 h, in 3 different days. Variations in the background air CO_2 mixing ratio and isotopic composition are likely to occur among sampling days but since the ‘Keeling plots’ include samples of high CO_2 mixing ratios, close to those of the end-member, the effect of variations in the background on the intercept is insignificant. Several additional exhaust samples were obtained a year later in a similar fashion through a 1/4 in. stainless steel tube inserted 15–40 cm into the tail pipe of the Ford Taurus (denoted ‘‘tail pipe CO_2 ,’’ Table 2). Human breath was sampled from four persons by exhaling through a $\text{Mg}(\text{ClO}_4)_2$ trap into pre-evacuated 500 ml flasks. For one of these persons, mixtures of ambient air and respired CO_2 were obtained by exhaling at various distances from the flask inlet.

In all cases, CO_2 was extracted from collected air, exhaust or breath within several hours of sampling by slowly expanding the sample into a glass vacuum line through four liquid N_2 traps. After all non-condensable gases were pumped away, liquid N_2 traps were warmed in series by three ethanol-dry ice traps and finally the fourth trap was thawed to room temperature, liberating the collected CO_2 . The carbon dioxide was then transferred into a calibrated volume, where its pressure was measured using an MKS Baratron, allowing us to calculate the number of moles of collected CO_2 . This number of moles was then re-calculated as CO_2 mixing ratio based on the known volumes of the sample flasks and measurements of pressure in the sample flasks prior to CO_2 extraction.

2.2. Isotopic analysis

The isotopic composition of extracted CO_2 was measured within 3 days of extraction by dual inlet gas source mass spectrometry using a Finnigan-MAT 253 isotope ratio mass spectrometer, configured to measure masses 44, 45, 46, 47, 48, and 49. A detailed description of the mass spectrometer is given by Eiler and Schauble (2004). Values of $\delta^{13}\text{C}$ and $\delta^{18}\text{O}$ were standardized by comparison with CO_2 generated by phosphoric acid digestion of NBS-19 and are reported vs. VPDB and VSMOW, respectively.

In reporting the abundance of mass 47 CO_2 we use the variable Δ_{47} , referred to here as the mass 47 anomaly. The anomaly for any isotopologue mass, i , Δ_i , is defined as the difference (in per mil) between the measured R^i ($=[\text{mass } i]/[\text{mass } 44]$, where i refers to masses 45, 46, or 47) and that ratio expected for CO_2 whose isotopes are distributed randomly among all isotopologues (Eiler and Schauble, 2004; Wang et al., 2004). Random distribution means that the abundance of an isotopologue is the product of the abundances of the isotopes it is composed of. For example, $[^{13}\text{C}^{18}\text{O}^{16}\text{O}]^* = 2[^{13}\text{C}][^{18}\text{O}][^{16}\text{O}]$, where * denotes the random distribution, and 2 is a symmetry number indicating that ^{18}O can sit in either of two equivalent positions. The randomly distributed abundance of mass 47 is then $[47]^* = [^{13}\text{C}^{18}\text{O}^{16}\text{O}]^* + [^{12}\text{C}^{18}\text{O}^{17}\text{O}]^* + [^{13}\text{C}^{17}\text{O}^{17}\text{O}]^*$ and Δ_{47} is defined as

$$\Delta_{47} = \left[\left(\frac{R^{47}}{R^{47*}} - 1 \right) - \left(\frac{R^{46}}{R^{46*}} - 1 \right) - \left(\frac{R^{45}}{R^{45*}} - 1 \right) \right] \times 1000, \quad (1)$$

where R^{47} , R^{46} , and R^{45} are measured values. R^{i*} for every sample is calculated from the measured R^{13} and R^{18} (see Eiler and Schauble, 2004, and Appendix B for more details and for an example of the calculation). R^{17} is calculated from R^{18} assuming the relationship $R^{17} = (R^{18}/R_{\text{VSMOW}}^{18})^{0.5164} \times R_{\text{VSMOW}}^{17}$, where R_{VSMOW}^{18} and R_{VSMOW}^{17} are taken as 0.0020052 and 0.0003799, respectively (Gonfiantini et al., 1993). Note that Δ_{47} values are only slightly sensitive to the power used to calculate R^{17} , with variation of $\pm 0.002\%$ in Δ_{47} for power between 0.5 and 0.528 (i.e., instead of 0.5164). Measure-

Table 1

CO₂ mixing ratios and isotopic composition in air, car exhaust, and breath samples (average $\pm 1\sigma$, $n = 3-6$, no error for samples measured once)

CO ₂ ($\mu\text{mol mol}^{-1}$)	$\delta^{13}\text{C}_{\text{VPDB}}$ (‰)	$\delta^{18}\text{O}_{\text{VSMOW}}$ (‰)	$\delta 47$ (‰)	Δ_{47} (‰)
<i>Exhaust air</i>				
22274	-24.205 ± 0.010	29.974 ± 0.025	6.868 ± 0.046	0.439 ± 0.051
19898	-24.105 ± 0.008	30.128 ± 0.013	7.060 ± 0.015	0.376 ± 0.032
3468	-22.803 ± 0.016	30.919 ± 0.026	9.250 ± 0.072	0.473 ± 0.044
3371	-22.885 ± 0.004	30.914 ± 0.005	9.102 ± 0.081	0.423 ± 0.073
3312 ^a	-22.898	29.093	7.236	0.383
1528	-20.276 ± 0.053	33.731 ± 0.116	14.715 ± 0.209	0.621 ± 0.042
1439	-20.371 ± 0.024	34.803 ± 0.025	15.712 ± 0.063	0.596 ± 0.047
776	-16.685 ± 0.003	36.092 ± 0.007	20.699 ± 0.027	0.658 ± 0.030
574	-13.413 ± 0.012	38.772 ± 0.019	26.704 ± 0.060	0.707 ± 0.032
437 ^a	-10.135	40.959	32.377	0.866
<i>Traffic air</i>				
446	-11.964	39.524	28.968	0.736
424	-10.933	40.542	31.073	0.777
420	-12.311	39.151	28.292	0.760
416	-10.313	41.188	32.417	0.848
412	-10.383	41.260	32.448	0.868
<i>Ambient air</i>				
404	-10.192 ± 0.033	41.883 ± 0.076	33.346 ± 0.075	0.956 ± 0.048
404	-10.001 ± 0.009	41.719 ± 0.010	33.128 ± 0.027	0.732 ± 0.040
401	-9.199 ± 0.011	41.579 ± 0.040	33.914 ± 0.073	0.841 ± 0.042
396	-9.653 ± 0.002	41.078 ± 0.033	32.977 ± 0.064	0.867 ± 0.032
384	-9.340 ± 0.004	40.599 ± 0.018	32.809 ± 0.063	0.871 ± 0.055
383	-9.769 ± 0.009	40.641 ± 0.018	32.461 ± 0.035	0.909 ± 0.007
<i>Human breath</i>				
30333 ^b	-23.086 ± 0.006	34.299 ± 0.016	12.632 ± 0.024	0.772 ± 0.006
29287 ^b	-21.875 ± 0.002	34.549 ± 0.002	14.153 ± 0.016	0.768 ± 0.015
19889 ^c	-23.121 ± 0.003	34.483 ± 0.008	12.793 ± 0.042	0.783 ± 0.033
7323 ^b	-21.015 ± 0.008	35.379 ± 0.017	15.971 ± 0.024	0.930 ± 0.033
5184 ^d	-21.201 ± 0.103	35.065 ± 0.216	15.212 ± 0.282	0.710 ± 0.038
5055 ^c	-20.678 ± 0.020	33.225 ± 0.080	13.861 ± 0.150	0.681 ± 0.114
1142 ^b	-17.358 ± 0.006	36.959 ± 0.009	20.952 ± 0.075	0.749 ± 0.002

All data are corrected for N₂O abundance. See Appendix B for an example of Δ_{47} and $\delta 47$ calculation procedure. Samples were collected between April and July 2004.

^a Exhaust air samples from Jeep Cherokee. The rest of exhaust samples are from Ford Taurus.

^b Breath of person 1. The samples of 7323 and 1142 $\mu\text{mol mol}^{-1}$ are mixtures of breath and ambient air instead of direct breath samples.

^{c,d,e} Breath from persons 2, 3, and 4 respectively.

Table 2

Isotopic composition of “tail pipe CO₂” collected at depths of 15–40 cm in the tail pipe of a Ford Taurus 2001 (average $\pm 1\sigma$, $n = 5-6$)

Depth in tail pipe (cm)	$\delta^{13}\text{C}_{\text{VPDB}}$ (‰)	$\delta^{18}\text{O}_{\text{VSMOW}}$ (‰)	Δ_{47} (‰)
15	-25.168 ± 0.002	29.737 ± 0.007	0.460 ± 0.044
20	-24.363 ± 0.004	30.624 ± 0.012	0.346 ± 0.029
25	-24.858 ± 0.005	29.993 ± 0.011	0.380 ± 0.047
30	-24.911 ± 0.011	29.893 ± 0.018	0.341 ± 0.057
40	-25.026 ± 0.008	30.374 ± 0.019	0.361 ± 0.031

All data are corrected for N₂O abundance. See Appendix B for an example of Δ_{47} calculation procedure. Samples were collected in June 2005.

ments of Δ_{47} are standardized by comparison with CO₂ that had been heated to 1000 °C for 2 h, driving it to the random distribution ($\Delta_{47} \equiv 0$).

Conservative mixing does not necessarily lead to linear trends in plots of Δ_{47} vs. $1/[\text{CO}_2]$ or vs. $\delta^{13}\text{C}$ or $\delta^{18}\text{O}$, for reasons discussed in Eiler and Schauble (2004), Zyakun

(2003), Kaiser et al. (2003), and in more detail in Appendix A of this work. Therefore, we find it useful to also report the $\delta 47$ value, which is defined here as $(R^{47}/R_{\text{std}}^{47} - 1) \times 1000$, where R_{std}^{47} is the R_{std}^{47} value for a hypothetical CO₂ whose $\delta^{13}\text{C}_{\text{VPDB}} = 0$, $\delta^{18}\text{O}_{\text{VSMOW}} = 0$, and $\Delta_{47} = 0$. Since $\delta 47$ is defined using the traditional delta notation, it produces linear trends in a ‘Keeling plot’ for conservative mixing processes (i.e., like $\delta^{13}\text{C}$ and $\delta^{18}\text{O}$).

The measured R^{47} value can be influenced by interferences from hydrocarbons and/or their fragmentation/recombination products (Eiler and Schauble, 2004). Therefore, prior to analysis the CO₂ was further purified by passing it through a Chrompack Poraplot-Q GC column, 25 m long, 0.32 μm ID, held at room temperature with 3 ml min⁻¹ helium as carrier. This purification method was later improved by using a Supelco QPlot column, 30 m long, 0.53 mm ID, held at -10 °C with 2 ml min⁻¹ helium as carrier and baked at 150 °C between samples. CO₂ was collected in a glass trap immersed in liquid N₂ at the end

of the column. The extent of remaining hydrocarbon contamination was estimated for each sample by monitoring the signal for mass 49, which is highly correlated with mass 47 excesses resulting from many contaminants (Eiler and Schauble, 2004). A sample was considered satisfactorily clean if there was no correlation between Δ_{47} values observed in five measurements and the difference in the mass 49 signal between sample and reference gas. This was typically obtained when the sample mass 49 signal was up to 0.5 mV (read through a $10^{12} \Omega$ resistor) higher than the reference gas signal. For car exhaust samples a cycle of GC cleaning as described above was typically not enough to bring the mass 49 signal of the sample to a satisfactorily low value and the CO_2 was typically passed a second time through the GC column (this was not necessary in the later improved GC method).

Mass spectrometry precision was typically 0.01‰ for $\delta^{13}\text{C}$, 0.03‰ for $\delta^{18}\text{O}$, 0.07‰ for $\delta 47$, and 0.04‰ for Δ_{47} (all 1σ) for a typical sample size of 50–100 μmol CO_2 that generated 10 V signal for mass 44 (read through a $3 \times 10^8 \Omega$ resistor) at typical instrumental conditions. This precision estimate was based on replicate mass spectrometry measurements of clean CO_2 . External precision for replicate air samples is poorer due to variable contamination and fractionation during sample preparation. We estimated this precision by replicate extractions of CO_2 from a cylinder of compressed air followed by GC removal of hydrocarbons and mass spectrometry. Δ_{47} was calculated for each mass spectrometer run, averaged for each sample (the standard deviation of this measurement gave the mass spectrometry precision), and compared among CO_2 samples to give external precision. External precision averaged 0.1‰ for $\delta^{13}\text{C}$, 0.3‰ for $\delta^{18}\text{O}$, 0.4‰ for $\delta 47$, and 0.07‰ for Δ_{47} . The precision in Δ_{47} measurements is better than that in $\delta 47$ since the errors due to fractionation in $\delta^{13}\text{C}$, $\delta^{18}\text{O}$, and $\delta 47$ are correlated.

All measurements of $\delta^{13}\text{C}$, $\delta^{18}\text{O}$, $\delta 47$, and Δ_{47} have been corrected for interferences from isotopologues of N_2O , which is not removed by our sample preparation method. The amount of N_2O in each sample was estimated by measuring the $\Delta 14$ value, defined as: $\Delta 14 = (V_{14_s} - V_{14_r}) / ((V_{44_s} + V_{44_r})/2)$, where V_{14} and V_{44} are the mass 14 and mass 44 voltages, respectively, and subscripts s and r refer to the sample and reference, respectively. The relationships between this variable and the isotopic values were calibrated by analyzing mixtures of N_2O and CO_2 prepared by freezing measured amounts of the pure gases together in liquid N_2 . N_2O corrections for air samples averaged $-0.19 \pm 0.03\%$ for $\delta^{13}\text{C}$, $-0.27 \pm 0.04\%$ for $\delta^{18}\text{O}$ (average $\pm 1\sigma$, $n = 7$), comparable to commonly used corrections (Mook and Jongsma, 1987; Mook and Van Der Hoek, 1983), $-0.34 \pm 0.05\%$ for $\delta 47$ and $+0.086 \pm 0.014\%$ for Δ_{47} . We also tested the efficacy of N_2O corrections based on measurements of mass 30 (i.e., $^{14}\text{N}^{16}\text{O}$). We compared N_2O correction using mass 14 to the correction using mass 30 by measuring air samples as well as the same

samples spiked with small amounts of N_2O . When corrected using mass 14 the isotopic values were similar in the original air sample and in the sample spiked with N_2O , whereas the correction based on mass 30 gave a significant deviation (probably because of a high mass 30 signal for CO_2 , possibly due to the presence of $^{12}\text{C}^{18}\text{O}$, as opposed to very low mass 14 signal). A potential problem in the use of mass 14 is interference due to trace amounts of N_2 in the sample. This was avoided by numerous steps (typically more than $10\times$) of freezing the CO_2 and N_2O in liquid nitrogen and pumping away any non-condensable gases. Furthermore, the integrity of the measurement was verified by observing $\Delta 14 = 0$ when measuring a standard containing no N_2O . Taking into account variations between -40 and $+40\%$ in $\delta^{15}\text{N}$ and between 20 and 60‰ in $\delta^{18}\text{O}$ values of N_2O (Rahn, 2005) would lead to a range of 0.02‰ in the possible N_2O correction for Δ_{47} . This is insignificant considering the precision of our measurement.

Gasoline was sampled at the Union 76 gasoline station, right after fueling the car used for most of the exhaust measurements (2001 Ford Taurus) by collecting several ml of gasoline from the same pump and immediately transferring it into closed glass vials. $\delta^{13}\text{C}$ in gasoline was measured by combustion in a Carlo Erba elemental analyzer (NA1500NC) attached to a Delta Plus Finnigan mass spectrometer at UC-Irvine. It is difficult to prevent evaporation of the gasoline samples while preparing the sample for measurement, and this might lead to fractionation of $\delta^{13}\text{C}$ values. To test the potential effect of evaporation, we measured samples of various sizes (1.3–2.3 mg) and samples were kept a variable amount of time (5–15 min) before measurement, allowing variable degrees of evaporation from the closed capsules (of up to $\sim 50\%$ evaporated). No significant differences in $\delta^{13}\text{C}$ were observed suggesting no significant fractionation in evaporation, consistent with data from Wang and Huang (2003) for C10 to C14 *n*-alkanes.

2.3. Statistical analysis

Estimated errors in sample handling and mass spectrometry analysis are given as the standard deviation about the mean (1σ). Statistical analyses of trends in ‘Keeling plots’ presented in Section 3 were made using the regression function in the data analysis add-in of Microsoft Excel X for Macintosh, where the error estimate for the concentrated end-member defined by the ‘Keeling plot’ trend is the standard error of the intercept. This analysis is a standard linear regression calculation that assumes no error associated with the x variable (model I, Miller and Tans, 2003; Pataki et al., 2003b). Regression calculation for ‘Keeling plot’ end-members is also performed using a second method, including uncertainty in the x variable (model II, assuming 1% error in the concentration values), according to the method of Reed (1992) by iterations using the Solver function in Microsoft Excel X for Macintosh.

3. Results and discussion

3.1. Car exhaust and urban air

Ambient air sampled on the Caltech campus varied in CO₂ mixing ratios from 383 to 404 $\mu\text{mol mol}^{-1}$, in $\delta^{13}\text{C}$ from -9.2 to -10.2‰ , in $\delta^{18}\text{O}$ from 40.6 to 41.9 ‰ , in $\delta 47$ from 32.5 to 33.9 ‰ , and in mass 47 anomaly (Δ_{47}) from 0.73 to 0.96 ‰ (Table 1 and see Appendix B for a detailed example of calculating Δ_{47} and $\delta 47$).

The CO₂ mixing ratios and bulk isotopic compositions ($\delta^{13}\text{C}$ and $\delta^{18}\text{O}$ values) observed in Pasadena ‘‘ambient’’ air were within the range of those previously observed in a several year record (Newman et al., 1999) and in spring 2003 measurements in the Los Angeles basin (Eiler and Schauble, 2004). The mixing ratios are higher and $\delta^{13}\text{C}$ values are lower than those of global background air (i.e., far from point sources or sinks). They are similar to those of suburban air in Paris (Widory and Javoy, 2003) and urban air in Dallas, Texas (Clark-Thorne and Yapp, 2003) and Krakow, Poland (Zimnoch et al., 2004), suggesting anthropogenic contributions even to the lowest mixing ratio samples. Values of $\delta^{18}\text{O}$ observed here are slightly higher than those observed in Salt Lake City, Utah (Pataki et al., 2003a). Values of Δ_{47} observed here are slightly higher, on average, than those observed in spring of 2003 in Pasadena (0.62–0.75 ‰ with one measurement of 0.93 ‰ ; Eiler and Schauble, 2004).

‘‘Traffic’’ air had consistently higher CO₂ mixing ratios, from 412 to 446 $\mu\text{mol mol}^{-1}$, similar to values observed in the streets of Paris (Widory and Javoy, 2003). It varied in $\delta^{13}\text{C}$ from -10.3 to -12.3‰ , in $\delta^{18}\text{O}$ from 39.2 to

41.2 ‰ , in $\delta 47$ from 28.3 to 32.5 ‰ , and in Δ_{47} from 0.74 to 0.87 ‰ .

‘‘Exhaust’’ air samples collected 30 or more cm from the car exhaust pipe varied in CO₂ mixing ratios from 574 to 3468 $\mu\text{mol mol}^{-1}$, in $\delta^{13}\text{C}$ from -13.4 to -22.8‰ , in $\delta^{18}\text{O}$ from 38.8 to 30.9 ‰ , in $\delta 47$ from 26.7 to 9.3 ‰ , and in Δ_{47} from 0.71 to 0.47 ‰ . Two samples obtained 5 cm below the car exhaust tail pipe had CO₂ mixing ratios of 2 and 2.2%, $\delta^{13}\text{C}$ of -24.2 and -24.1‰ , $\delta^{18}\text{O}$ of 30.0 and 30.1 ‰ , $\delta 47$ of 6.9 and 7.1 ‰ , and Δ_{47} of 0.44 and 0.38 ‰ .

These three groups of samples (‘‘Ambient,’’ ‘‘Traffic,’’ and ‘‘Exhaust’’) were used together to derive the isotopic composition of the CO₂ emitted from cars using a ‘Keeling plot’ mass balance approach (Fig. 1). When analyzing the plot by standard linear regression (model I), the intercept for the trend defined by all measurements, reflecting the car exhaust end-member, is characterized by a $\delta^{13}\text{C}$ value of $-24.4 \pm 0.2\text{‰}$, $\delta^{18}\text{O}$ of $29.9 \pm 0.4\text{‰}$, $\delta 47$ of $6.6 \pm 0.6\text{‰}$, and Δ_{47} of $0.41 \pm 0.03\text{‰}$ (intercept \pm SE). No significant change was observed in the end-member values when the regression calculation included uncertainty in the x variable (see Appendix A). We therefore use the above values in the following discussion. Δ_{47} is not linear in simple mixing but for mixing of car exhaust into air this non-linearity has only a small effect (smaller than the precision analysis) which we ignore in the following discussion (see Appendix A for details).

The $\delta^{13}\text{C}$ of CO₂ in car exhaust primarily depends on the fuel used. Petroleum used to produce gasoline varies in $\delta^{13}\text{C}$ between -29.9 and -31.5‰ for non-marine sources, and between -23.1 and -32.5‰ for marine sources (Yeh and Epstein, 1981), with a global weighted average

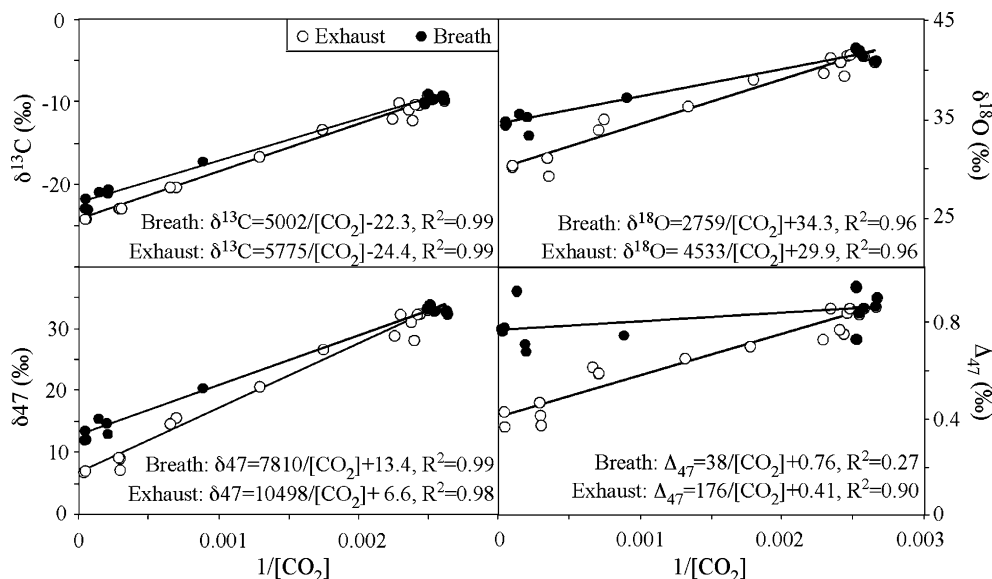


Fig. 1. ‘Keeling plots’ for $\delta^{13}\text{C}$ (vs. VPDB), $\delta^{18}\text{O}$ (vs. VSMOW), $\delta 47$ and Δ_{47} in CO₂. $[\text{CO}_2]$ is the CO₂ mixing ratio in $\mu\text{mol mol}^{-1}$. Empty symbols refer to CO₂ in air mixed with car exhaust obtained by sampling at varying distance from car exhaust pipe as well as air at a busy junction and ‘‘ambient’’ air in the Caltech campus in Pasadena, CA. Bold symbols refer to human breath samples and air mixed with human breath. The obtained ‘Keeling plot’ trends were $\delta^{13}\text{C} = 5775/[\text{CO}_2] - 24.4$, $\delta^{18}\text{O} = 4533/[\text{CO}_2] + 29.9$, $\delta 47 = 10498/[\text{CO}_2] + 6.6$, and $\Delta_{47} = 176/[\text{CO}_2] + 0.41$ for car exhaust, and $\delta^{13}\text{C} = 5002/[\text{CO}_2] - 22.3$, $\delta^{18}\text{O} = 2759/[\text{CO}_2] + 34.3$, $\delta 47 = 7810/[\text{CO}_2] + 13.4$, and $\Delta_{47} = 38/[\text{CO}_2] + 0.76$ for human breath. See Appendix A for a discussion on linearity approximation for the Δ_{47} mixing line.

estimated to be -26.5‰ (Andres et al., 2000; Tans, 1981). The $\delta^{13}\text{C}$ of the gasoline used to fill the tank of the car used for most of our “Exhaust” data points was measured to be $-24.4 \pm 0.2\text{‰}$ ($n = 4$), in agreement with the car exhaust end-member defined by our data. This value is higher than those typically observed for gasoline (Clark-Thorne and Yapp, 2003; Pataki et al., 2003a; Widory and Javoy, 2003) but is similar to that observed in Poland (-25‰ , Zimnoch et al., 2004) and can be explained by the mixture of sources of petroleum products used in California (approximately half local sources, and the rest Alaskan and imported oil; Sally Newman, personal communication, 2005). Most urban air measurements result in an anthropogenic end-member that is lower in $\delta^{13}\text{C}$ than gasoline due to the contribution of CO_2 produced from combustion of natural gas (Pataki et al., 2003a; Takahashi et al., 2002; Zondervan and Meijer, 1996 and Sally Newman, personal communication, 2005). However, when measured in streets with significant automobile traffic, as in the case of our “Traffic” and “Exhaust” measurements, the anthropogenic end-member closely approaches the $\delta^{13}\text{C}$ of local gasoline (Widory and Javoy, 2003).

In global models of the isotopic budget of CO_2 , its $\delta^{18}\text{O}$ value is dominated by exchange with plant and soil water, and the anthropogenic component is generally neglected (Ishizawa et al., 2002). In urban air and in some continental stations, however, the anthropogenic component is likely to be significant. The $\delta^{18}\text{O}$ of CO_2 produced in combustion is generally assumed to equal that of atmospheric oxygen (Ciais et al., 1997; Pataki et al., 2003a; Peylin et al., 1999; Zimnoch et al., 2004; Zondervan and Meijer, 1996); that is, 23.8‰ (Coplen et al., 2002; although 23.5‰ (Kroopnick and Craig, 1972) is used in most studies of urban CO_2 sources). In Salt Lake city, the weighted average $\delta^{18}\text{O}$ values of urban CO_2 sources, at times when combustion of either gasoline or natural gas is expected to be the dominant source, were found to be slightly lower than this value (21.9‰ for rush hour measurements and 23.1‰ for winter nights). The difference was attributed to a contribution from soil respiration (Pataki et al., 2003a). In Pasadena, on the other hand, the weighted average $\delta^{18}\text{O}$ of urban CO_2 sources has been estimated at 27‰ (Newman et al., 1999). This value is closer to our car exhaust end-member ($29.9 \pm 0.4\text{‰}$), but still significantly lower. In this case, the difference might reflect contributions from natural gas combustion, producing CO_2 with a $\delta^{18}\text{O}$ equal to that of O_2 in air, or from soil respiration, which we estimate should have a $\delta^{18}\text{O}$ of approximately 24‰ (local tap water is -9‰ , Lisa Welp, personal communication, 2004; and soil respiration flux should be approximately 7‰ lower than equilibrium with this water, Miller et al., 1999).

We expected CO_2 produced in car exhaust to have a Δ_{47} value close to zero as was observed in one of two car exhaust samples measured by Eiler and Schauble (2004), because it is generated by combustion at temperatures of at least 900 °C . Instead, the measured Δ_{47} value of $0.41 \pm 0.03\text{‰}$ is consistent with the equilibrium distribu-

tion of isotopologues at $195 \pm 15\text{ °C}$ (Wang et al., 2004). We suggest this reflects isotopic re-equilibration of CO_2 in the car exhaust stream, mediated by exchange with water, as detailed in the following paragraph.

Isotopic exchange among isotopologues of pure gaseous CO_2 is slow relative to the timescales of exhaust production and emission, even at temperatures of up to several hundred degree celsius. However, in the presence of condensed water (at near ambient temperatures) or water vapor (at elevated temperatures), re-equilibration of CO_2 isotopologues is far faster, presumably facilitated by $\text{CO}_2\text{-H}_2\text{O}$ exchange. In this case, CO_2 re-equilibration must be accompanied by changes in its $\delta^{18}\text{O}$ value, by an amount that depends on the relative amounts of CO_2 and H_2O , and the temperature of exchange. The temperature dependency of oxygen isotopic fractionation between CO_2 and liquid H_2O is summarized in Friedman and O’Neil (1977, Data from Figs. 5 and 6 of that reference up to 300 °C were used to estimate fractionation at higher temperatures by fitting a second order polynomial of $1/T$ (K) and extrapolating to high temperature by forcing the fractionation factor to zero at $1/T = 0$, giving a correlation of $R^2 = 0.999$). The fractionation between CO_2 and water vapor ($\epsilon_{\text{CO}_2\text{-H}_2\text{O}}$ in Eq. (2)) has not been previously measured at temperatures relevant to our calculation, but can be estimated as the sum of the fractionation factors in exchange between CO_2 and liquid water, and in evaporation of water (values for water evaporation are taken from curve A in Fig. 8 in Friedman and O’Neil, 1977 and are forced to zero above the critical point of 374 °C). The resulting gas-phase fractionation factor at $195 \pm 15\text{ °C}$ (the temperature of re-equilibration implied by the Δ_{47} value of exhaust CO_2) is $20.5 \pm 1.3\text{‰}$. If we assume that gasoline combustion is the only source of water in the exhaust gas (and that water and CO_2 are the only oxygen bearing combustion products present in significant amounts), we can use the stoichiometry of the components of gasoline to estimate the relative amount of CO_2 and H_2O in the exhaust gas and therefore of the distribution of oxygen used in combustion between CO_2 and H_2O . The C/H ratio of gasoline (0.56, estimated from the weighted average stoichiometry of the components of gasoline, Na et al., 2004) implies that the fraction of oxygen atoms, which is present in CO_2 ($X_{\text{O-CO}_2} = 2C/(2C + 0.5H)$), is 0.69. We further assume that all oxygen in both CO_2 and H_2O comes from O_2 in air, and thus that the weighted average $\delta^{18}\text{O}$ of the exhaust stream is 23.8‰ . Given these constraints and assumptions, we can calculate the oxygen isotope mass balance for CO_2 and H_2O in the exhaust stream using the relationship

$$\begin{aligned} \delta^{18}\text{O}_{\text{O}_2} &= X_{\text{O-CO}_2} \delta^{18}\text{O}_{\text{CO}_2} + X_{\text{O-H}_2\text{O}} \delta^{18}\text{O}_{\text{H}_2\text{O}} \\ &= X_{\text{O-CO}_2} \delta^{18}\text{O}_{\text{CO}_2} \\ &\quad + (1 - X_{\text{O-CO}_2}) \frac{(\delta^{18}\text{O}_{\text{CO}_2} - \epsilon_{\text{CO}_2\text{-H}_2\text{O}})}{\left(\frac{\epsilon_{\text{CO}_2\text{-H}_2\text{O}}}{1000} + 1\right)}. \end{aligned} \quad (2)$$

Substituting the constraints quoted above into this relationship yields a predicted $\delta^{18}\text{O}$ for CO₂ in exhaust of between 30.6‰ (for re-equilibration at 210 °C) and 31.6‰ (for re-equilibration at 180 °C), which closely approaches the measured $\delta^{18}\text{O}$ value of the car exhaust end-member (Fig. 2). We conclude that both the Δ_{47} and $\delta^{18}\text{O}$ values of CO₂ in car exhaust can be understood as a consequence of isotopic re-equilibration between CO₂ and H₂O in the exhaust stream, quenching at ca. 200 °C. The exhaust does not cool to such a temperature until it exits the catalytic converter, and so presumably this quenching occurs between the downstream side of the catalytic converter and the tail pipe.

Alternatively, both Δ_{47} and $\delta^{18}\text{O}$ values in the car exhaust may also be explained by only partial exchange with exhaust water at a lower temperature. For example, a mixture of approximately equal proportions of CO₂ equilibrated at 900 °C with CO₂ re-equilibrated at 50 °C (the temperature of the exhaust at the exit of the tail pipe) would yield Δ_{47} and $\delta^{18}\text{O}$ values consistent with a temperature of ~ 200 °C. In an attempt to resolve these two alternative interpretations, we sampled exhaust gas at depths of 15–40 cm within the tail pipe (Table 2). These measurements were performed a year after the above data were obtained, when gasoline composition was potentially different, and are therefore not included in the ‘Keeling plots’. We anticipate that if the measured Δ_{47} reflects full exchange at 200 °C, we should find a constant Δ_{47} and $\delta^{18}\text{O}$ in all parts of the tail pipe having temperatures lower than 200 °C. In contrast, if the measured Δ_{47} reflects mixing of high and low temperature gas, we should find a gradient of increasing Δ_{47} and $\delta^{18}\text{O}$ with decreasing temperature of collection, or values near $\Delta_{47} = 0$ ‰ at all temperatures above the partial exchange temperature. We found that at depths up to

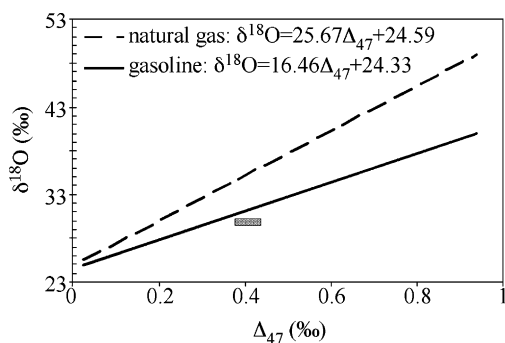


Fig. 2. Correlation between Δ_{47} and $\delta^{18}\text{O}$ (vs. VSMOW) of CO₂ produced in combustion and undergoing isotopic exchange with water produced in combustion at different temperatures. $\delta^{18}\text{O}$ was estimated by a mass balance of the oxygen atoms (Eq. (2)) using the isotopic fractionation factor in ¹⁸O exchange between CO₂ and water vapor, estimated as the sum of the fractionation factors in water evaporation and CO₂ exchange with liquid water (raw data from Friedman and O’Neil, 1977) and a fraction of oxygen atoms in CO₂ estimated from the stoichiometry of chemical components of gasoline (Na et al., 2004) and methane (as representing natural gas). Full line depicts gasoline and dashed line depicts methane. The gray rectangle depicts the range of car exhaust end-members from Fig. 1.

40 cm, corresponding to collection temperatures up to 70 °C, Δ_{47} varied between 0.34 ± 0.06 ‰ and 0.46 ± 0.04 ‰, and $\delta^{18}\text{O}$ varied from 29.7 ± 0.01 ‰ to 30.6 ± 0.01 ‰ with no clear spatial gradient (Table 2). Although inconclusive, these results support the interpretation that CO₂ is homogeneously reset to ~ 200 °C. Note that exchange in sample flasks after sampling would result in a Δ_{47} value of approximately 0.95‰, irrespective of the amount of water available, inconsistent with our results.

As opposed to the two cars measured in this work, one sample measured previously (Eiler and Schauble, 2004) had lower values for both Δ_{47} and $\delta^{18}\text{O}$ (0.06 ± 0.08 ‰ and 24.24 ± 0.18 ‰, respectively). These lower values are consistent with Eq. (2) for the expected combustion temperatures ($\Delta_{47} = 0.06 \pm 0.08$ ‰ corresponds to approximately 700 °C with the error bars between 450 °C and more than 1000 °C). It is conceivable that cars of different engine designs and possibly even different driving conditions would have different re-equilibration temperatures and therefore different values for both Δ_{47} and $\delta^{18}\text{O}$, though we expect that these two isotopic tracers should stay correlated through Eq. (2). In other words, when incorporating Δ_{47} values into isoflux models one should not use a single value for Δ_{47} and for $\delta^{18}\text{O}$ of combustion, but an equation that ties both tracers together (Fig. 2).

Furthermore, it seems likely that other combustion processes, such as natural gas combustion in a power plant where the path of the flue gas in the chimney is different than that of car exhaust, could lead to different re-equilibration temperatures and different combined Δ_{47} – $\delta^{18}\text{O}$ signatures following Eq. (2). We use Eq. (2) to calculate the $\delta^{18}\text{O}$ of the CO₂ in equilibrium with water produced in combustion of natural gas ($X_{\text{O-CO}_2} = 0.50$ based on the stoichiometry of methane). The higher hydrogen content of natural gas yields additional water in combustion, thus leading to a higher $\delta^{18}\text{O}$ value for the CO₂ at any given exchange temperature (Fig. 2). Therefore, Δ_{47} and $\delta^{18}\text{O}$ of CO₂ produced in combustion should be included together in models not as constant values but through equations describing the relationships between these two tracers, where different kinds of fuel (i.e., gasoline and natural gas) would each have a specific equation.

3.2. Human breath

The CO₂ mixing ratios in breath samples of four individuals varied between 0.5 and 3% (Table 1). These breath samples varied in $\delta^{13}\text{C}$ from -20.7 to -23.1 ‰, in $\delta^{18}\text{O}$ from 33.2 to 35.1‰, in Δ_{47} from 0.68 to 0.78‰, and in δ_{47} from 12.7 to 15.2‰. Mixing lines between human breath and background air on a ‘Keeling plot’ were used to estimate respiratory end-members. Mixing lines for $\delta^{13}\text{C}$, $\delta^{18}\text{O}$, and δ_{47} were largely similar to those obtained for car exhaust mixing into air (Fig. 1), with standard linear regression calculations (model I) yielding end-member values of -22.3 ± 0.2 ‰, 34.3 ± 0.3 ‰, and 13.4 ± 0.4 ‰, respectively. Δ_{47} in breath samples, on the other hand,

was not significantly different than that of background air, averaging $0.74 \pm 0.05\%$ (average $\pm 1\sigma$).

CO₂ in human and animal breath is typically slightly lower in $\delta^{13}\text{C}$ than body organic matter, which in turn is slightly higher in $\delta^{13}\text{C}$ than dietary carbon (De Niro and Epstein, 1978). Therefore, variations in breath $\delta^{13}\text{C}$ among individuals and regions are likely to be due to variations in diet. Values of $\delta^{13}\text{C}$ observed here are within the range previously observed in this region (Epstein and Zeiri, 1988) and are similar to those observed recently in the area (Eiler and Schauble, 2004) and to an experiment of controlled diet based on C₃ plants but supplemented with C₄ glucose (Pantelev et al., 1999). The values we observe are slightly higher than the values observed in Paris, France (-24.5% , Widory and Javoy, 2003), suggesting that the diet in Southern California is slightly higher in $\delta^{13}\text{C}$ than that in France, possibly due to a larger contribution of C₄ plants to the Californian diet.

The $\delta^{18}\text{O}$ value of CO₂ in animal breath is in equilibrium with body water, and is approximately 38‰ higher than body water (Luz et al., 1984), which in turn is related to drinking water (Luz et al., 1984). The $\delta^{18}\text{O}$ values observed here for human breath are within the range observed in the past in the region (Eiler and Schauble, 2004; Epstein and Zeiri, 1988) and close to the value expected based on local tap water $\delta^{18}\text{O}$ of approximately -9% .

Eiler and Schauble (2004) observed a preliminary value for Δ_{47} in human breath of 0.66% , slightly lower than the value observed in the current study (0.74%). The current value of 0.74% is closer to, though still slightly lower than the value predicted based on equilibrium with water at body temperature (0.89% predicted for 37 °C, Wang et al., 2004), suggesting that Δ_{47} values of human breath, and possibly other respiration processes, are affected by an additional unknown process and do not carry a pure equilibrium signal. The key for our purposes, however, is that Δ_{47} in breath is within measurement error of that in ambient air samples and differs significantly from that of car exhaust.

The $\delta^{13}\text{C}$ of respiration (as exemplified by human breath) is similar to that of CO₂ produced by combustion and is therefore not very useful in distinguishing between the two CO₂ sources. Values of $\delta^{18}\text{O}$ could be used to separate respiration from combustion sources, although the respiration source is expected to vary substantially with the $\delta^{18}\text{O}$ of local meteoric water, and in many regions overlaps the $\delta^{18}\text{O}$ we observe here for car exhaust, again making it difficult to de-convolve the two sources using $\delta^{18}\text{O}$. Values of δ_{47} , the variable newly defined here, should be highly correlated with $\delta^{18}\text{O}$ in combustion and respiration sources. In contrast, the mass 47 anomaly (Δ_{47}) for CO₂ that undergoes exchange with water at ambient temperatures, as in human, plant, and soil respiration, is predicted to vary only due to equilibrium temperature (Wang et al., 2004), and to be uniformly high (ca. 0.8%) compared to combustion sources (0.4% for exhaust in this study; 0.0% for natural gas combustion in Eiler and Schauble (2004)). Thus, the isotopic index Δ_{47} can be used to distin-

guish CO₂ from combustion sources vs. respiration sources (and other sources involving low-temperature isotopic equilibration with water).

Acknowledgments

We thank Xiaomei Xu of UC-Irvine for measurements of the $\delta^{13}\text{C}$ of gasoline, and Sally Newman, Lisa Welp, and Zhengrong Wang for helpful discussions as well as James Farquhar, Jan Kaiser, and two anonymous reviewers for constructive comments and suggestions. This work is supported by Grants NSF-EAR-0091842, NSF-EAR-0220066, and NSF-EAR-0345905.

Associate editor: James Farquhar

Appendix A. Non-linearity of trends in ‘Keeling plots’ based on Δ_{47}

The ‘Keeling plot’ approach for finding mixture end-members in air relies on the linearity of the delta scale to mixing. However, conservative mixing leads to non-linear variations in mass 47 anomaly (Eiler and Schauble, 2004). In this appendix, we examine this problem in detail for mixtures between CO₂ end-members having bulk stable isotope compositions similar to those of natural sources. First, samples of CO₂ having a range of initial bulk stable isotope compositions were heated to 1000 °C, to drive their Δ_{47} values to 0.0% . We describe these samples as ‘heated gases.’ We then prepared a second set of samples of CO₂ having a range of initial bulk stable isotope compositions by exposing them to liquid water at room temperature for several days to drive their Δ_{47} value toward the room-temperature equilibrium of ca. 0.9% . We describe these samples as ‘non-heated gases.’

Fig. 3A shows the isotopic compositions of various mixtures of a heated and a non-heated gas that were similar to one another in bulk stable isotope composition ($\delta^{13}\text{C}$ values of -34.0 and -33.9% ; $\delta^{18}\text{O}$ values of 4.0 and 4.9% ; Δ_{47} values of 0.907 and 0%). Fig. 3B shows the isotopic compositions of various mixtures of a heated and a non-heated gas that were strongly different from one another in bulk stable isotope composition ($\delta^{13}\text{C}$ values of -3.6 and -33.4% ; $\delta^{18}\text{O}$ values of 39.7 and 5.7% ; Δ_{47} values of 0.828 and 0%).

Data trends in Figs. 3A and B are compared to two types of calculated mixing lines: one that assumes conservative linear mixing of Δ_{47} values (incorrect, but a useful visual reference), and a second that assumes linear mixing of the measured delta values ($\delta^{13}\text{C}$, $\delta^{18}\text{O}$ as well as raw δ_{45} , δ_{46} , and δ_{47} values) and then calculates the Δ_{47} value of each mixture based on these mass balance predicted delta values. When the two end-members are similar in bulk isotopic composition, no significant difference is observed between the two mixing lines; that is, Δ_{47} values can be treated as if they were a conservative tracer in mixing problems (Fig. 3A, note that the two mixing lines fall on top of

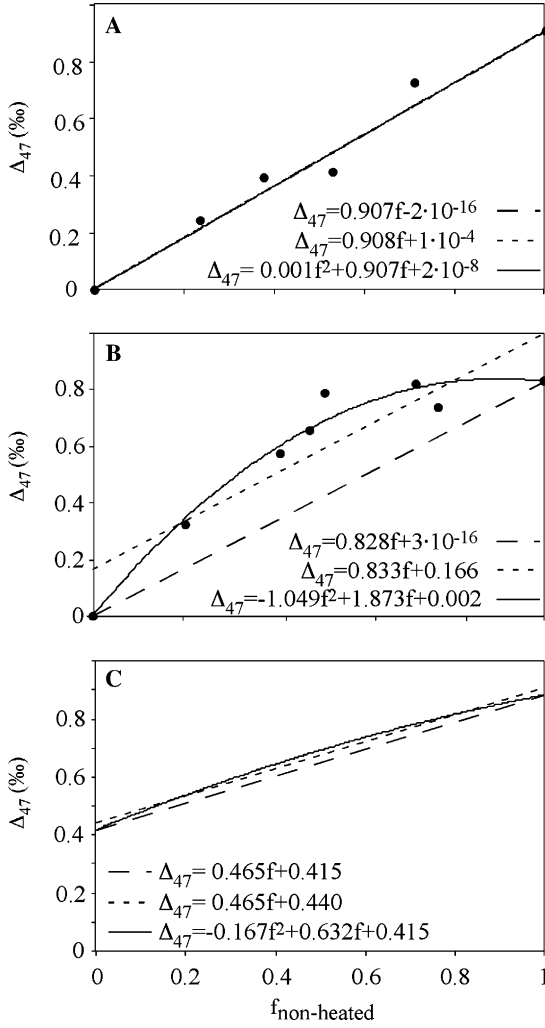


Fig. 3. Nonlinearity of Δ_{47} in mixing. Curves are calculated mixing lines using heated ($\Delta_{47} = 0$) and non-heated end-members ($\Delta_{47} = 0.907$ in (A) and 0.828 in (B)). Long dashed line is the mixing line assuming conservative mixing of Δ_{47} values. Full line is a polynomial fit to the fully calculated Δ_{47} (assuming linearity in measured δ values but not in mass 47 anomaly). Short dashed line is a linear fit to fully calculated Δ_{47} . Bold circles are measured Δ_{47} values. (A) Mixing lines for end-members similar in $\delta^{13}\text{C}$ and $\delta^{18}\text{O}$ (note that all lines seem as one as they are practically identical for this mixture). (B) Mixing lines for end-members of different $\delta^{13}\text{C}$ and $\delta^{18}\text{O}$. (C) Arithmetic mixing of car exhaust with average “ambient” air.

each other). However, when the two end-members differ in bulk isotopic composition, the mixing line for Δ_{47} deviates significantly from linear (Fig. 3B). If one were to fit a straight line through the data (or the correctly calculated mixing curve), one would erroneously conclude that the heated end-member has a Δ_{47} value of 0.166 ± 0.083 , rather than the actual value of 0.0‰ . The actual trend can be reasonably well fitted using a second order polynomial.

A similar approach was used to estimate the deviation from linearity in the mixing of car exhaust into air, in which the difference in bulk composition between the two end-members is smaller than that in Fig. 3B. The car

exhaust sample of highest mixing ratio was arithmetically mixed with an average air sample to obtain the mass balance predicted $\delta^{13}\text{C}$, $\delta^{18}\text{O}$ as well as δ_{45} , δ_{46} , δ_{47} values and the fully calculated Δ_{47} values (as above), and compared to the mass balance predicted Δ_{47} (assuming linearity in conservative mixing of Δ_{47} values). The difference between fully calculated Δ_{47} and that calculated assuming linearity reached a maximum of 0.042‰ , for the 1:1 mixture (Fig. 3C).

As with the artificial mixture (Fig. 3B), the fully calculated Δ_{47} in Fig. 3C can also be fitted with a second order polynomial function, whose intercept reflects the correct Δ_{47} of car exhaust end-member. The difference between the end-member obtained using the polynomial fit and that obtained using a linear fit to the fully calculated Δ_{47} was 0.025‰ ($\Delta_{47} = 0.39\text{‰}$ for the polynomial fit). This deviation from linearity is too small to be observed in Fig. 1, since it is at the limit of the measurement accuracy. However, applying a mass balance approach to future air sample analysis, as is done for $\delta^{13}\text{C}$ and $\delta^{18}\text{O}$, would likely require improved accuracy than is currently available and would then also require considering the non-linearity of Δ_{47} .

The non-linearity is explained by the mathematical behavior of Δ_{47} in a mass balance treatment. Δ_{47} is defined and calculated as

$$\Delta_{47} = \left[\left(\frac{R^{47}}{R^{47*}} - 1 \right) - \left(\frac{R^{46}}{R^{46*}} - 1 \right) - \left(\frac{R^{45}}{R^{45*}} - 1 \right) \right] \times 1000, \quad (\text{A1})$$

where R^{47} , R^{46} , and R^{45} are the ratio values of 47/44, 46/44, and 45/44 as derived from the measured δ_{47} , δ_{46} , and δ_{45} for each sample (see Appendix B for an example of the calculation). R^{47*} , R^{46*} , and R^{45*} are the corresponding ratio values calculated assuming random distribution among isotopologues and are derived as follows:

$$\begin{aligned} R^{45*} &= R^{13} + 2R^{17}, \\ R^{46*} &= 2R^{18} + 2R^{13} \times R^{17} + (R^{17})^2, \\ R^{47*} &= 2R^{13} \times R^{18} + 2R^{17} \times R^{18} + R^{13} \times (R^{17})^2, \end{aligned} \quad (\text{A2})$$

where R^{13} and R^{18} are derived from the measured $\delta^{13}\text{C}$ and $\delta^{18}\text{O}$, and R^{17} is derived from R^{18} , assuming mass dependent relation between them. Then

$$\Delta_{47} = \left[\frac{R^{47}}{2R^{13} \times R^{18} + 2R^{17} \times R^{18} + R^{13} \times (R^{17})^2} - \frac{R^{46}}{2R^{18} + 2R^{13} \times R^{17} + (R^{17})^2} - \frac{R^{45}}{R^{13} + 2R^{17}} + 1 \right] \times 1000. \quad (\text{A3})$$

The ‘Keeling plot’ method is based on mass balance using

$$c_a = c_b + c_s \quad \text{and} \quad \delta_a c_a = \delta_b c_b + \delta_s c_s, \quad (\text{A4})$$

where c_a is the amount of CO₂ (depicted as mixing ratio) in an air sample, c_b is the amount of CO₂ in an air parcel of background atmosphere, and c_s is the amount of CO₂ added by

the studied source, in this case by car exhaust. δ_a , δ_b , and δ_s are the respective δ values. The combination results in

$$\delta_a = \frac{c_b}{c_a}(\delta_b - \delta_s) + \delta_s \quad (\text{A5})$$

that is traditionally plotted as δ_a as a function of $1/c_a$ (as in Fig. 1) but can also be plotted as a function of c_b/c_a , which is the fraction of background air in the measured air (defined as f in Fig. 3).

This mass balance approach can be applied to Δ_{47} by transforming Eq. (A5) to ratios

$$R_a = f(R_b - R_s) + R_s \quad (\text{A6})$$

and substituting Eq. (A6) to each of the ratios comprising Eq. (A3)

$$\begin{aligned} \Delta_{47} = & \{ (f(R_a^{47} - R_s^{47}) + R_s^{47}) / [2(f(R_a^{13} - R_s^{13}) + R_s^{13}) \\ & \times (f(R_a^{18} - R_s^{18}) + R_s^{18}) + 2(f(R_a^{17} - R_s^{17}) + R_s^{17}) \\ & \times (f(R_a^{18} - R_s^{18}) + R_s^{18}) + (f(R_a^{13} - R_s^{13}) + R_s^{13}) \\ & \times (f(R_a^{17} - R_s^{17}) + R_s^{17})^2] - (f(R_a^{46} - R_s^{46}) + R_s^{46}) \\ & / [2(f(R_a^{18} - R_s^{18}) + R_s^{18}) + (f(R_a^{17} - R_s^{17}) + R_s^{17})^2] \\ & + 2(f(R_a^{13} - R_s^{13}) + R_s^{13})(f(R_a^{17} - R_s^{17}) + R_s^{17}) \\ & - (f(R_a^{45} - R_s^{45}) + R_s^{45}) / [(f(R_a^{13} - R_s^{13}) + R_s^{13}) \\ & + 2(f(R_a^{17} - R_s^{17}) + R_s^{17})] + 1 \} \times 1000. \quad (\text{A7}) \end{aligned}$$

This cannot be expressed as a simple function of f and must be approximated by expanding it to a polynomial series. The examples shown in Figs. 3B and C indicate that the third and fourth order coefficients are negligible, suggesting that Δ_{47} vs. f can be approximated as a second order polynomial fit, in which the intercept equals Δ_{47-s} . Fitting a second order polynomial to the Δ_{47} car exhaust ‘Keeling plot’ yields an end-member value of 0.39‰ ($\Delta_{47} = -20515[\text{CO}_2]^{-2} + 232.3[\text{CO}_2]^{-1} + 0.39$, $R^2 = 0.907$).

End-members can be estimated from the ‘Keeling plots’ also by a regression analysis that takes into account measurement errors in both the isotopic composition (the errors are given in Table 1) and mixing ratios (estimated as 1% of the value). This yielded end-member values of -24.4‰ , 29.7‰ , 6.3‰ , and 0.38‰ for $\delta^{13}\text{C}$, $\delta^{18}\text{O}$, $\delta 47$, and Δ_{47} , respectively. For human breath ‘Keeling plots’ this regression analysis yielded end-member values of -23.3‰ , 34.5‰ , 13.6‰ , and 0.72‰ for $\delta^{13}\text{C}$, $\delta^{18}\text{O}$, $\delta 47$, and Δ_{47} , respectively. In both cases, these values are not significantly different from standard regression analysis (as reported in the body of the text).

Appendix B. An example of calculating Δ_{47} and $\delta 47$

To illustrate the methodology for calculation of Δ_{47} and $\delta 47$, we will present here a detailed example of such calculations for one sample (one of the mass spectrometry runs for the 4th ambient air sample in Table 1). From the mass spectrometric measurement we obtain raw values for $\delta 45$,

$\delta 46$, and $\delta 47$. For this sample these values were -5.678 , 1.510 , and -4.237‰ , respectively, relative to our working reference gas whose $\delta^{13}\text{C}_{\text{VPDB}} = -3.698\text{‰}$ and $\delta^{18}\text{O}_{\text{VSMOW}} = 39.272\text{‰}$ (as determined by NBS-19 measurements). An ^{17}O correction was performed based on $R^{17} = R_{\text{VSMOW}}^{17}(R^{18}/R_{\text{VSMOW}}^{18})^{0.5164}$, where $R_{\text{VSMOW}}^{17} = 0.00037995$ and $R_{\text{VSMOW}}^{18} = 0.0020052$ (Gonfiantini et al., 1993), by varying R^{13} and R^{18} (using the Solver function in Excel) to yield a minimal value to the function $(R^{13} + 2R^{18} - R^{45})^2 + (2R^{18} + 2R^{13}R^{17} + (R^{17})^2 - R^{46})^2$. The resulting $\delta^{13}\text{C}_{\text{VPDB}}$ and $\delta^{18}\text{O}_{\text{VSMOW}}$ values were -9.801 and 40.856‰ , respectively.

The values of $\delta^{13}\text{C}$ and $\delta^{18}\text{O}$ were then used to calculate R^{13} and R^{18} resulting in 0.0111271 and 0.0020871 , respectively (using $R_{\text{VPDB}}^{13} = 0.0112372$ and $R_{\text{VSMOW}}^{18} = 0.0020052$). R^{17} was then calculated as above resulting in 0.00038784 . The abundance of each one of the isotopes was calculated as: $[^{12}\text{C}] = (1 + R^{13})^{-1} = 0.9889954$, $[^{13}\text{C}] = R^{13}/(1 + R^{13}) = 0.0110046$, $[^{16}\text{O}] = (1 + R^{17} + R^{18})^{-1} = 0.9975311$, $[^{17}\text{O}] = R^{17}/(1 + R^{17} + R^{18}) = 0.00038688$, $[^{18}\text{O}] = R^{18}/(1 + R^{17} + R^{18}) = 0.0020820$. These abundance values are used to calculate the randomly distributed abundance of the CO_2 isotopologues: $[44]^* = [12][16][16] = 0.9841181$, $[45]^* = [13][16][16] + 2[12][16][17] = 0.011714$, $[46]^* = 2[12][16][18] + [12][17][17] + 2[13][16][17] = 0.0041166$, $[47]^* = 2[13][16][18] + [13][17][17] + 2[12][17][18] = 4.7304 \times 10^{-5}$. The randomly distributed isotopic ratios are then calculated by dividing the respective abundance by $[44]^*$, yielding $R^{45*} = 0.0119027$, $R^{46*} = 0.0041830$, and $R^{47*} = 4.8068 \times 10^{-5}$. The same calculations were done for the reference gas, yielding $R_{\text{ref}}^{45*} = 0.011780$, $R_{\text{ref}}^{46*} = 0.0041101$, and $R_{\text{ref}}^{47*} = 4.7510 \times 10^{-5}$. Then, the measured isotopic ratios for the samples are obtained from $R^i = (\delta i/1000 + 1) \times R_{\text{ref}}^i$, where i refers to masses 45, 46, and 47, and $\Delta_{47} = [(R^{47}/R^{47*} - 1) - (R^{46}/R^{46*} - 1) - (R^{45}/R^{45*} - 1)] \times 1000 = 0.143\text{‰}$.

The values are then corrected for the presence of N_2O with $\Delta_{14} = 0.00273$. The calibration slopes were -62.3 , -89.6 , and 28.7 for $\delta^{13}\text{C}$, $\delta^{18}\text{O}$, and Δ_{47} , respectively, resulting in $\delta^{13}\text{C} = -9.631\text{‰}$, $\delta^{18}\text{O} = 41.100\text{‰}$, and $\Delta_{47} = 0.065\text{‰}$. Next, the Δ_{47} value obtained was normalized using a standard whose $\Delta_{47} = 0$ by definition, which was produced by heating CO_2 to 1000 °C for 2 h to obtain random distribution of the isotopologues. Δ_{47} obtained for this heated gas standard was $\Delta_{47} = -0.824\text{‰}$, and the normalized sample value is therefore $\Delta_{47} = 0.065 - (-0.824) = 0.889\text{‰}$. Each sample was typically measured three times and the values were averaged. For this sample this resulted in $\delta^{13}\text{C} = -9.653\text{‰}$, $\delta^{18}\text{O} = 41.078\text{‰}$, and $\Delta_{47} = 0.867\text{‰}$ as in Table 1.

The scale of $\delta 47$ was defined here as $\delta 47 = (R^{47}/R_{\text{std}}^{47} - 1) \times 1000$, where R_{std}^{47} is the R^{47} value for a hypothetical CO_2 whose $\delta^{13}\text{C}_{\text{VPDB}} = 0$, $\delta^{18}\text{O}_{\text{VSMOW}} = 0$, and $\Delta_{47} = 0$. R^{47*} for the measured heated gas and the hypothetical zero standard were calculated as described above, resulting in $R_{\text{heated}}^{47*} = 4.8248 \times 10^{-5}$ and $R_{\text{zero}}^{47*} = 4.6591 \times 10^{-5}$. The measured $\delta 45$, $\delta 46$, and $\delta 47$ of the sample were corrected as

well for N₂O presence using calibration slopes of -59.9 , -84.6 , and -113.7 for $\delta 45$, $\delta 46$, and $\delta 47$, respectively, resulting in $\delta 45 = -5.515\text{‰}$, $\delta 46 = 1.741\text{‰}$, and $\delta 47 = -3.927\text{‰}$. The calibrated sample $\delta 47$ was then calculated as $[(\delta 47/1000 + 1)/(\delta 47_{\text{heated}}/1000 + 1) \times (R_{\text{heated}}^{47*}/R_{\text{zero}}^{47*}) - 1] \times 1000 = 30.022\text{‰}$ ($\delta 47_{\text{heated}}$ was -1.475‰) and the averaged value for the mass spectrometer measurements of this sample was 32.977‰ .

References

- Andres, R.J., Marland, G., Boden, T., Bischof, S., 2000. Carbon dioxide emissions from fossil fuel consumption and cement manufacture, 1751–1991, and an estimate of their isotopic composition and latitudinal distribution. In: Wigley, T.M.L., Schimel, D.S. (Eds.), *The Carbon Cycle*. Cambridge University Press, Cambridge, pp. 53–62.
- Ciais, P., Denning, A.S., Tans, P.P., Berry, J.A., Randall, D.A., Collatz, G.J., Sellers, P.J., White, J.W.C., Trolier, M., Meijer, H.A.J., Francey, R.J., Monfray, P., Heimann, M., 1997. A three-dimensional synthesis study of $\delta^{18}\text{O}$ in atmospheric CO₂. 1. Surface fluxes. *Journal of Geophysical Research-Atmospheres* **102** (D5), 5857–5872.
- Ciais, P., Tans, P.P., Trolier, M., White, J.W.C., Francey, R.J., 1995a. A large northern-hemisphere terrestrial CO₂ sink indicated by the $^{13}\text{C}/^{12}\text{C}$ ratio of atmospheric CO₂. *Science* **269** (5227), 1098–1102.
- Ciais, P., Tans, P.P., White, J.W.C., Trolier, M., Francey, R.J., Berry, J.A., Randall, D.R., Sellers, P.J., Collatz, J.G., Schimel, D.S., 1995b. Partitioning of ocean and land uptake of CO₂ as inferred by $\delta^{18}\text{O}$ measurements from the NOAA Climate Monitoring and Diagnostics Laboratory Global Air Sampling Network. *Journal of Geophysical Research-Atmospheres* **100** (D3), 5051–5070.
- Clark-Thorne, S.T., Yapp, C.J., 2003. Stable carbon isotope constraints on mixing and mass balance of CO₂ in an urban atmosphere: Dallas metropolitan area, Texas, USA. *Applied Geochemistry* **18** (1), 75–95.
- Coplen, T.B., Hopple, J.A., Bohlke, J.K., Peiser, H.S., Rieder, S.E., Krouse, H.R., Rosman, K.J.R., Ding, T., Vocke Jr, R.D., Revesz, K.M., Lambert, A., Taylor, P., De Bièvre, P., 2002. Compilation of minimum and maximum isotope ratios of selected elements in naturally occurring materials and reagents, US Geological Survey Water-Resources Investigations Report 01-4222. pp. 38.
- Cuntz, M., Ciais, P., Hoffmann, G., Allison, C.E., Francey, R.J., Knorr, W., Tans, P.P., White, J.W.C., Levin, I., 2003. A comprehensive global three-dimensional model of $\delta^{18}\text{O}$ in atmospheric CO₂: 2. Mapping the atmospheric signal. *Journal of Geophysical Research-Atmospheres* **108** (D17), art. no.-4528.
- De Niro, M.J., Epstein, S., 1978. Influence of diet on distribution of carbon isotopes in animals. *Geochimica et Cosmochimica Acta* **42** (5), 495–506.
- Eiler, J.M., Schauble, E., 2004. $^{18}\text{O}^{13}\text{C}^{16}\text{O}$ in earth's atmosphere. *Geochimica et Cosmochimica Acta* **68** (23), 4767–4777.
- Epstein, S., Zeiri, L., 1988. Oxygen and carbon isotopic compositions of gases respired by humans. *Proceedings of the National Academy of Sciences of the United States of America* **85** (6), 1727–1731.
- Francey, R.J., Tans, P.P., 1987. Latitudinal variation in O-18 of atmospheric CO₂. *Nature* **327** (6122), 495–497.
- Francey, R.J., Tans, P.P., Allison, C.E., Enting, I.G., White, J.W.C., Trolier, M., 1995. Changes in oceanic and terrestrial carbon uptake since 1982. *Nature* **373** (6512), 326–330.
- Friedman, I., O'Neil, J.R., 1977. Compilation of stable isotope fractionation factors of geological interest. In: *Data of Geochemistry*, 6th ed. Geological Survey Professional Paper 440-KK.
- Gonfiantini, R., Stichler, W., Rozanski, K., 1993. Standards and intercomparison materials distributed by the international atomic energy agency for stable isotope measurements. In: *Reference and Intercomparison Materials for Stable Isotopes of Light Elements*, pp. 13–29. IAEA-TECDOC-825.
- Ishizawa, M., Nakazawa, T., Higuchi, K., 2002. A multi-box model study of the role of the biospheric metabolism in the recent decline of $\delta^{18}\text{O}$ in atmospheric CO₂. *Tellus Series B-Chemical and Physical Meteorology* **54** (4), 307–324.
- Kaiser, J., Rockmann, T., Brenninkmeijer, C.A.M., 2003. Assessment of $^{15}\text{N}^{15}\text{N}^{16}\text{O}$ as a tracer of stratospheric processes. *Geophysical Research Letters* **30** (2), doi:10.1029/2002GL016253.
- Keeling, C.D., 1958. The concentration and isotopic abundances of atmospheric carbon dioxide in rural areas. *Geochimica et Cosmochimica Acta* **13** (4), 322–334.
- Keeling, C.D., 1961. The concentration and isotopic abundances of carbon dioxide in rural and marine air. *Geochimica et Cosmochimica Acta* **24** (3-4), 277–298.
- Kroopnick, P., Craig, H., 1972. Atmospheric oxygen—isotopic composition and solubility fractionation. *Science* **175** (4017), 54–55.
- Luz, B., Kolodny, Y., Horowitz, M., 1984. Fractionation of oxygen isotopes between mammalian bone phosphate and environmental drinking water. *Geochimica et Cosmochimica Acta* **48** (8), 1689–1693.
- Miller, J.B., Tans, P.P., 2003. Calculating isotopic fractionation from atmospheric measurements at various scales. *Tellus Series B-Chemical and Physical Meteorology* **55** (2), 207–214.
- Miller, J.B., Yakir, D., White, J.W.C., Tans, P.P., 1999. Measurement of $^{18}\text{O}/^{16}\text{O}$ in the soil-atmosphere CO₂ flux. *Global Biogeochemical Cycles* **13** (3), 761–774.
- Mook, W.G., Jongasma, J., 1987. Measurement of the N₂O correction for $^{13}\text{C}/^{12}\text{C}$ ratios of atmospheric CO₂ by removal of N₂O. *Tellus Series B—Chemical and Physical Meteorology* **39**, 96–99.
- Mook, W.G., Van der Hoek, S., 1983. The N₂O correction in the carbon and oxygen isotopic analysis of atmospheric CO₂. *Isotope Geoscience* **1** (3), 237–242.
- Na, K., Kim, Y.P., Moon, I., Moon, K.C., 2004. Chemical composition of major VOC emission sources in the Seoul atmosphere. *Chemosphere* **55** (4), 585–594.
- Newman, S., Xu, X., Rodrigues, C., Epstein, S., Stolper, E., 1999. Concentrations and isotopic ratios of CO₂ in air in the Los Angeles basin as measures of pollution. *Eos Trans. AGU*, 80, Fall meeting supplement, Abstract A52D-05.
- Pantelev, N., Peronnet, F., Hillaire-Marcel, C., Lavoie, C., Massicotte, D., 1999. Carbon isotope fractionation between blood and expired CO₂ at rest and exercise. *Respiration Physiology* **116** (1), 77–83.
- Pataki, D.E., Bowling, D.R., Ehleringer, J.R., 2003a. Seasonal cycle of carbon dioxide and its isotopic composition in an urban atmosphere: anthropogenic and biogenic effects. *Journal of Geophysical Research-Atmospheres* **108** (D23), Art. no.-4735.
- Pataki, D.E., Ehleringer, J.R., Flanagan, L.B., Yakir, D., Bowling, D.R., Still, C.J., Buchmann, N., Kaplan, J.O., Berry, J.A., 2003b. The application and interpretation of Keeling plots in terrestrial carbon cycle research. *Global Biogeochemical Cycles* **17** (1), Art. no.-1022.
- Peylin, P., Ciais, P., Denning, A.S., Tans, P.P., Berry, J.A., White, J.W.C., 1999. A 3-dimensional study of $\delta^{18}\text{O}$ in atmospheric CO₂: contribution of different land ecosystems. *Tellus Series B—Chemical and Physical Meteorology* **51** (3), 642–667.
- Rahn, T., 2005. Factors influencing the stable isotopic content of atmospheric N₂O. In: Flanagan, L.B., Ehleringer, J.R., Pataki, D.E. (Eds.), *Stable Isotopes and Biosphere-atmosphere Interactions: Processes and Biological Control*. Elsevier Academic Press, New York, pp. 268–287.
- Reed, B.C., 1992. Linear least-squares fits with errors in both coordinates. 2. Comments on parameter variances. *American Journal of Physics* **60** (1), 59–162.
- Takahashi, H.A., Konohira, E., Hiyama, T., Minami, M., Nakamura, T., Yoshida, N., 2002. Diurnal variation of CO₂ concentration, $\Delta^{14}\text{C}$ and $\delta^{13}\text{C}$ in an urban forest: estimate of the anthropogenic and biogenic CO₂ contributions. *Tellus Series B-Chemical and Physical Meteorology* **54** (2), 97–109.

- Tans, P.P., 1981. $^{13}\text{C}/^{12}\text{C}$ of industrial CO_2 . In: Bolin, B. (Ed.), *SCOPE 16: Carbon Cycle Modelling*. Wiley, New York, pp. 127–129.
- Wang, Y., Huang, Y.S., 2003. Hydrogen isotopic fractionation of petroleum hydrocarbons during vaporization: implications for assessing artificial and natural remediation of petroleum contamination. *Applied Geochemistry* **18** (10), 1641–1651.
- Wang, Z., Schauble, E.A., Eiler, J.M., 2004. Equilibrium thermodynamics of multiply-substituted isotopologues of molecular gases. *Geochimica et Cosmochimica Acta* **68** (23), 4779–4797.
- Widory, D., Javoy, M., 2003. The carbon isotope composition of atmospheric CO_2 in Paris. *Earth and Planetary Science Letters* **215** (1–2), 289–298.
- Yakir, D., Wang, X.F., 1996. Fluxes of CO_2 and water between terrestrial vegetation and the atmosphere estimated from isotope measurements. *Nature* **380** (6574), 515–517.
- Yeh, H.W., Epstein, S., 1981. Hydrogen and carbon isotopes of petroleum and related organic matter. *Geochimica et Cosmochimica Acta* **45** (5), 753–762.
- Zimnoch, M., Florkowski, T., Necki, J., Neubert, R., 2004. Diurnal variability of $\delta^{13}\text{C}$ and $\delta^{18}\text{O}$ of atmospheric CO_2 in the urban atmosphere of Krakow, Poland. *Isotopes in Environmental and Health Studies* **40** (2), 129–143.
- Zondervan, A., Meijer, H.A.J., 1996. Isotopic characterization of CO_2 sources during regional pollution events using isotopic and radiocarbon analysis. *Tellus Series B-Chemical and Physical Meteorology* **48** (4), 601–612.
- Zyakun, A.M., 2003. What factors can limit the precision of isotope ratio measurements in the isotopomer pool? *International Journal of Mass Spectrometry* **229** (3), 217–224.